Please cite this article as:
Ewa Węgrzyn-Skrzypczak, Tomasz Skrzypczak, Numerical analysis of the solidification process with natural convection of the liquid phase, Scientific Research of the Institute of Mathematics and Computer Science, 2006, Volume 5, Issue 1, pages 185-190.
The website: http://www.amcm.pcz.pl/

NUMERICAL ANALYSIS OF THE SOLIDIFICATION PROCESS WITH NATURAL CONVECTION OF THE LIQUID PHASE

Ewa Węgrzyn-Skrzypczak[1], Tomasz Skrzypczak[2]

[1] *Institute of Mathematics and Computer Science, Czestochowa University of Technology, Poland*
[2] *Institute of Mechanics and Machine Design, Czestochowa University of Technology, Poland*

Abstract. The paper deals with numerical modeling of binary alloys solidification process with motion of the fluid in the liquid and mushy zone. The mathematical model of the phenomenon is presented. Finite Element Method is used for modeling process. The results of the numerical simulation in the 2D region are discussed.

1. Mathematical model

Solidifying region is divided into three subregions (Fig. 1) with different physical properties. The liquid area Ω_L is filled with moving liquid alloy, the area Ω_S contains non-moving solid material and Ω_{L+S} is filled with mixture of liquid and solid phases.

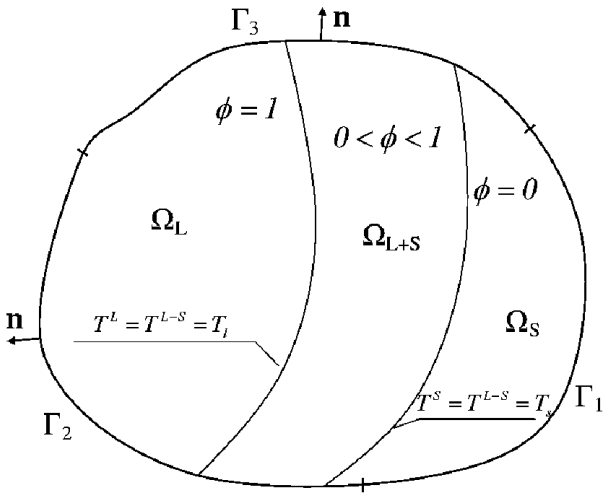

Fig. 1. Considered domain divided into liquid, mushy and solid zone

Mathematical model consists of heat transport equation with convection term, momentum equation with buoyancy and Darcy's drag term and continuity equation

$$c^*(T)\left(\frac{\partial T}{\partial t}+u_i T_{,i}\right)=(\lambda T_{,i})_{,i} \tag{1}$$

$$\frac{\mu}{\rho}u_{i,jj}-u_j u_{i,j}-\frac{1}{\rho}p_{,i}-\frac{\mu}{\rho K}u_i-\delta_{ij}g_i\beta(T-T_{ref})=\frac{\partial u}{\partial t} \tag{2}$$

$$u_{i,i}=0 \tag{3}$$

The value of the artificial heat capacity c^* is calculated based on the following relation [3]

$$c^*(T)=\begin{cases} c_s\rho_s, & T<T_s \\ \frac{1}{2}(c_s\rho_s+c_l\rho_l)-\rho_s L\frac{\partial[1-\phi(T)]}{\partial T}, & T_s\le T\le T_l \\ c_l\rho_l, & T>T_l \end{cases} \tag{4}$$

where $\phi(T)$ is porosity coefficient defined as

$$\phi(T)=\begin{cases} 0, & T<T_s \\ \frac{T-T_s}{T_l-T_s}, & T_s\le T\le T_l \\ 1, & T>T_l \end{cases} \tag{5}$$

Equations (1)-(3) are completed by the Dirichlet, Neumann and Newton boundary conditions

$$\boldsymbol{X}\in\Gamma_1 : T=T_b \tag{6}$$

$$\boldsymbol{X}\in\Gamma_2 : -\lambda\boldsymbol{n}\cdot\boldsymbol{grad}T=q_b \tag{7}$$

$$\boldsymbol{X}\in\Gamma_3 : -\lambda\boldsymbol{n}\cdot\boldsymbol{grad}T=\alpha(T-T_\infty) \tag{8}$$

and following initial conditions

$$\boldsymbol{X}\in\Gamma_{1-3} : u_i=0 \tag{9}$$

$$t=0 : T=T_0,\quad u_i=0 \tag{10}$$

Permeability of the porous region is calculated based on Karman-Kozeny relation [2]

$$K=\frac{{d_p}^2\phi^3(T)}{180(1-\phi(T))^2} \tag{11}$$

where d_p is average pore diameter depending on the size of the forming grains. Material properties are averaged using following formula

$$\begin{aligned} \rho &= \phi(T)\rho_l + [1-\phi(T)]\rho_s \\ \lambda &= \phi(T)\lambda_l + [1-\phi(T)]\lambda_s \end{aligned} \tag{12}$$

2. Numerical model

The weighted residual method for the heat transport equation (1) is introduced

$$\int_\Omega w\left[\lambda T_{,ii} - c^*(T)\left(\frac{\partial T}{\partial t} + u_i T_{,i}\right)\right] d\Omega = 0 \tag{13}$$

Weak form of (13) is presented

$$\lambda\int_\Omega w_{,i}\, T_{,i}\, d\Omega + c^*\int_\Omega w u_i T_{,i}\, d\Omega + c^*\int_\Omega w\frac{\partial T}{\partial t} d\Omega = \oint_\Gamma w q_b d\Gamma \tag{14}$$

Equation (14) is discretized over space using Petrov-Galerkin method. For the finite element one can write

$$\lambda\int_{\Omega^{(e)}} w_{i,k}\, N_{j,k}\, d\Omega^{(e)} + c^*\int_{\Omega^{(e)}} w_i N_j u_k^j N_{l,k}\, d\Omega^{(e)} + c^*\int_{\Omega^{(e)}} w_i N_j d\Omega^{(e)} = \oint_{\Gamma^{(e)}} w_i q_b d\Gamma^{(e)} \tag{15}$$

where N_i is linear shape function of the finite element and w_i can be written as follows

$$w_i = N_i + \gamma_i \frac{h_i}{2}\frac{\left(u_k^i N_{i,k}\right)}{\left|u^i\right|} \tag{16}$$

where

$$\gamma_i = \operatorname{ctg} h(Pe_i) - \frac{1}{Pe_i} \tag{17}$$

$$Pe_i = \frac{\rho c\left|u^i\right| h_i}{2\lambda} \tag{18}$$

Integral terms from (15) can be written in the following matrix form:

$$\boldsymbol{K}^{(e)} = \lambda\int_{\Omega^{(e)}} w_{i,k}\, N_{j,k}\, d\Omega^{(e)} \tag{19}$$

$$\boldsymbol{A}^{(e)} = c^* \int_{\Omega^{(e)}} w_i N_j u_k^j N_{l,k} \, d\Omega^{(e)} \tag{20}$$

$$\boldsymbol{M}^{(e)} = c^* \int_{\Omega^{(e)}} w_i N_j d\Omega^{(e)} \tag{21}$$

$$\boldsymbol{B}^{(e)} = \oint_{\Gamma^{(e)}} w_i q_b d\Gamma^{(e)} \tag{22}$$

where $\boldsymbol{K}^{(e)}$ is element heat conductivity matrix, $\boldsymbol{A}^{(e)}$ - advection matrix, $\boldsymbol{M}^{(e)}$ - heat capacity matrix and $\boldsymbol{B}^{(e)}$ - right hand side vector.
After procedure of discretization over time (Euler backward scheme) and agregation of the discrete model we obtain global finite element equation

$$\left(\boldsymbol{K} + \boldsymbol{A} + \frac{1}{\Delta t} \boldsymbol{M} \right) \boldsymbol{T}^{f+1} = \frac{1}{\Delta t} \boldsymbol{M} \boldsymbol{T}^{f} + \boldsymbol{B} \tag{23}$$

We solve Navier-Stokes equation (2) by a characteristic based split (CBS) scheme based on the projection metod of Chorin [1] as described in Zienkiewicz and Codina [4] and Zienkiewicz and Taylor [5]. In this metod an auxiliary velocity field $\boldsymbol{u}^*$ is introduced to uncouple equations (2) and (3):

$$\begin{aligned} \Delta u_i^* = u_i^* - u_i^f = \Delta t \Bigg[& \frac{\mu}{\rho} u_{i,jj} - u_j u_{i,j} - \frac{\mu}{\rho K} u_i - \delta_{ij} g_i \beta (T - T_{ref}) + \\ & + \frac{\Delta t}{2} u_{i,i} \left[u_j u_{i,j} + \delta_{ij} g_i \beta \left(T - T_{ref} \right) \right] \Bigg]_{t=t^f} \end{aligned} \tag{24}$$

The final velocity field is corrected by the pressure increment so that is divergence free:

$$u_i^{f+1} - u_i^* = \frac{\Delta t}{\rho} \left(p_{,i} \right)^{f+1} \tag{25}$$

By taking the divergence of (25) we arrive at the following Poisson equation for the pressure:

$$\Delta t \left(p_{,ii} \right)^{f+1} = \rho u_i^*{}_{,i} \tag{26}$$

We apply the standard Galerkin procedure for (24)-(26).

3. Example of the numerical simulation

The computer simulation of the solidification process of the casting in the sand mould was made. The boundary and initial conditions are presented in the picture.

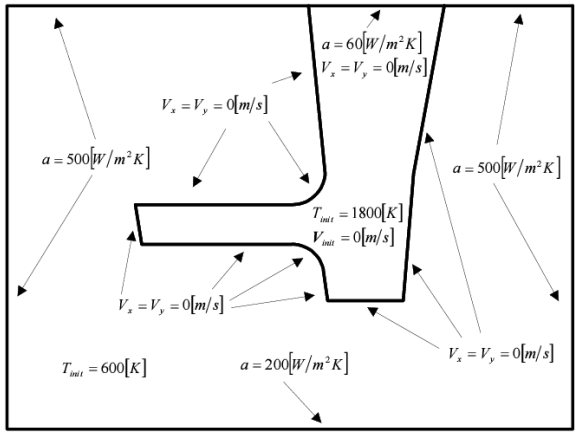

Fig. 2. Boundary and initial conditions

In Figure 3 we can see velocity field after 50, 250 and 550 s. The movement of the liquid alloy can be observed in the liquid and porous region.

After 50 s we observe convection cells in the pure liquid region (Fig. 3a). The rest of the casting is filled with porous material. Velocities in this area are smaller than in the central region of the casting.

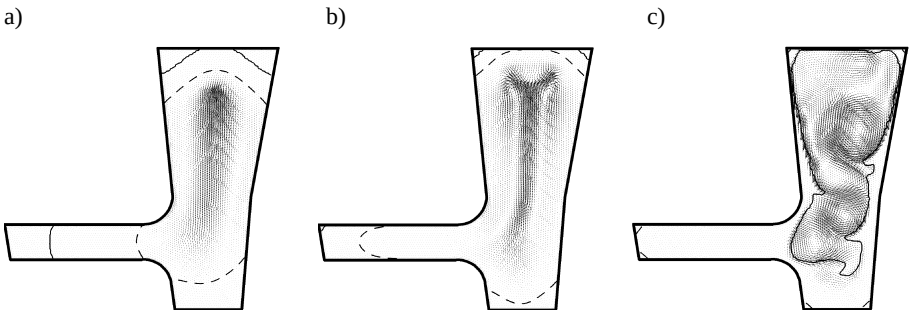

Fig. 3. Three stages of solidification process in the casting

After 250 s pure liquid region is vanished and the entire area of the casting is filled with mixture of the liquid and solid (Fig. 3b). We can see the stream of the liquid material which flows from the bottom to the top of the casting. On the top it divides into two streams.

After 550 s there are pure solid areas in the corners of the casting. The rest of the solidifying region contains porous material. The motion of the fluid slowly vanishes due to solid fraction continuous growth.

Conclusions

Analysing the results of the numerical simulation it can be concluded that wide mushy region appears in the casting solidifying in the sand mould. The material properties of the sand mould guarantees low cooling rates, so the mushy zone can evolute so easily. Low cooling rates in the casting favours equiaxed solidification.

References

[1] Chorin A.J., Numerical solution of the Navier-Stokes equation, Math. Comput. 1968, 23, 745-762.

[2] Kaviany M., Principles of heat transfer in porous media, Springer-Verlag, New York Inc. 1991.

[3] Mochnacki B., Suchy J.S., Numerical methods in computations of foundry processes, Polish Foundrymen's Technical Association, Kraków 1995.

[4] Zienkiewicz O.C., Codina R., A general algorithm for compressible and incompressible flow, Part I. The split characteristic based scheme, International Journal for Numerical Metods in Fluids 1995, 20, 869-885.

[5] Zienkiewicz O.C., Taylor R.L., The finite element method, Volume 3: Fluid dynamics, Butterworth and Hienemann 2000.